International Journal of Pharmaceutics 697 (2026) 126871

Contents lists available at ScienceDirect

International Journal of Pharmaceutics

journal homepage: www.elsevier.com/locate/ijpharm

Accurate low-temperature direct granule extrusion 3D printing of personalised paediatric minitablets

Bambang V.E.B. Abdillah Akbar [a], Michalina Seluk [b], Abdullah Isreb [c], Marcelo da Silva [a], Cécile A. Dreiss [a], Paul G. Royall [a], Andrea Gill [d], Louise Bracken [d], Stephen Tomlin [e], Joanna Giebułtowicz [b], Stuart A. Jones [a,f], Mohamed A. Alhnan [a,f,*]

[a] Institute of Pharmaceutical Science, King's College London, London SE1 9NH, UK
[b] Faculty of Pharmacy, Medical University of Warsaw, Warsaw, Poland
[c] School of Pharmacy and Biomolecular Sciences, Liverpool John Moores University, Liverpool L3 3AF, UK
[d] Paediatric Medicines Research Unit, Alder Hey Children's NHS Foundation Trust, Liverpool L12 2AP, UK
[e] Pharmacy Department, Great Ormond Street Hospital for Children NHS Foundation Trust, London WC1N 3JH, UK
[f] Centre for Pharmaceutical Medicine Research (CPMR), Institute of Pharmaceutical Science, King's College London, London SE1 9NH, UK

ARTICLE INFO

Keywords:
Additive manufacturing
Robust production
Precision medicine
Paediatric-friendly
Individualised therapy

ABSTRACT

Medicine individualisation remains constrained by the limited availability of age-appropriate strengths and by extemporaneous practices that can compromise dose consistency. Direct extrusion 3D printing offers an alternative manufacturing method for personalised medicine, without introducing solvents, complex preparation, or post-processing that challenge the adoption in pharmacy. However, achieving uniform weight and drug content in small objects (e.g., paediatric-friendly minitablets) and lowering the preparation temperature remain challenges for direct extrusion-based 3D printing technologies.

In this work, we introduce a facile low-temperature direct granules extrusion 3D printing strategy to manufacture carvedilol minitablets, starting from carvedilol powder or crushed licensed tablets as starting materials, using a high-precision pharmaceutical-grade 3D printer. Methacrylate-based polymers, polyethylene glycol, and glyceryl monostearate were used to enable extrusion at 70–75°C. When the 3D printer was challenged with minute-dimensional designs, it was possible to manufacture batches of minitablets up to 2 mm in diameter with 0.8 mm in thickness. The lowest minitablet weight variation was 1.48%, achieved with an optimal diameter of 3.6 mm and a thickness of 1.6 mm; this was also reflected in the drug content uniformity (within ± 5%). The batches also met British Pharmacopoeia requirements for dissolution (>80% in 45 min).

These findings extend direct extrusion 3D printing to a viable manufacturing platform for accurate, low-dose small solid units, such as minitablets. By coupling a GMP-compliant 3D printer with a simplified preparation workflow, this work provides a realistic blueprint for integrating direct extrusion-enabled personalised minitablets into hospital pharmacy and point-of-care settings.

1. Introduction

Children exhibit a wide range of body physiologies, including weight, height, body composition, and organ development, which leads to different pharmacokinetic profiles of drugs (Khan et al., 2022; Taylor et al., 2024). Only about a quarter of the approved indications by the FDA Centre for Drug Evaluation and Research (CDER) for new drugs were designated for patients under 18 years old (Kakkilaya et al., 2025). As a result, conversion of the existing dosage forms is commonly performed to adjust paediatric acceptance and doses, but this approach has raised several problems, including preparation error, dose accuracy, consistency, and stability (Abu-Geras et al., 2017; Kasahun and Sendekie, 2023; Paulsson et al., 2025). The most widely used off-label forms, oral liquid solutions and suspensions, may pose a palatability issue due to the lack of taste masking and/or flavouring agents for bitter-taste medicine and dose accuracy issue (Galande et al., 2020; Neves and

* Corresponding author at: Centre for Pharmaceutical Medicine Research, Institute of Pharmaceutical Science, King's College London, 150 Stamford Street, London SE1 9NH, UK.
E-mail address: alhnan@kcl.ac.uk (M.A. Alhnan).

https://doi.org/10.1016/j.ijpharm.2026.126871
Received 30 January 2026; Received in revised form 10 April 2026; Accepted 11 April 2026
Available online 13 April 2026

Auxtero, 2021).

Age-appropriate solid preparations in multiparticulate forms, including minitablets, are more suitable in most cases, given their promising dose accuracy and taste-masking effect (Meyers, 2024; Rouaz et al., 2021; Zuccari et al., 2022). Minitablet, tablet with a diameter of 2–4 mm (Lennartz and Mielck, 1998; Meruva et al., 2024), has been recommended by the European Medicines Agency (EMA) as an exemplary formulation for children (EMA, 2013). Several exploratory studies worldwide have shown that minitablets are accepted by children (Duncan et al., 2026; Klingmann et al., 2013; Miyazaki et al., 2022; Spomer et al., 2012). Minitablets are conventionally manufactured on a large scale using a tablet rotary press with specialised punches and dies, which lacks personalisation and requires excellent properties of powder (Flemming and Mielck, 1995; Kachrimanis et al., 2005; Loo et al., 2023; Lura et al., 2025).

Personalising tablets is an attractive application for additive (Auel et al., 2025) and subtractive manufacturing (Kaba et al., 2023; Liu et al., 2023). Several reports indicated the potential of high accuracy 3D printing technologies for manufacturing bespoke minitablets, such as digital light processing (DLP) and drop-on-demand (DOD) (Adamov et al., 2022; Sundarkumar et al., 2023). However, DLP technology utilises photo initiators, raising safety and toxicity concerns about residues in the final product, while DOD requires post-processing to remove residual solvent, which may not be practical in a clinical setting (Cui et al., 2021; Ghazali et al., 2023; Kim et al., 2022). Extrusion-based methods offer safer excipient options, but they suffer from unsatisfactory printing resolution of minitablets less than 50 mg in weight. Semi-solid extrusion (SSE) often exhibits lower printing resolution and greater weight variation than others (3.12–20.73%) (Ayyoubi et al., 2025; Eduardo et al., 2021; Hu et al., 2023; Protopapa et al., 2024), largely because semi-solid feeds can spread after deposition, and because SSE frequently operates with larger nozzle diameters to maintain shape fidelity and avoid clogging (Aina et al., 2025). In contrast, fused deposition modelling (FDM) commonly uses narrow nozzles and thin-layer thickness control at high temperature, which can enable finer feature definition and lower weight deviation (1.6–17.46%) (Gorkem Buyukgoz et al., 2022; Krause et al., 2021). Meanwhile, direct extrusion has been reported to exhibit unsatisfactory weight uniformity (RSD $>$ 5%), even with a small nozzle size (0.2 mm) (Fratini et al., 2025).

Direct extrusion offers a significant advantage over FDM and SSE, as it is filament-free and solvent-free, thereby gaining production efficiency and minimising stability issues (Bernatoniene et al., 2025; Milliken et al., 2024). One essential parameter in the direct extrusion process is the printing temperature, which affects the extrudability of the ink. In the printing sample compartment, solids require higher temperatures to change their viscoelastic behaviour to the point of extrusion. Therefore, plasticisers and/or lubricants are often added to reduce the matrix glass temperature (Aguilar-de-Leyva et al., 2024; Waterman and Adami, 2005). Previous attempts at minitablet production via direct extrusion reported printing temperatures at 170–180°C using PVA-HPMC and HPC polymers with PEG 6000 as a plasticiser (Fratini et al., 2025; Totaro et al., 2025). With regular-sized tablets, only two studies produced direct extrusion tablets at 80–95°C using Eudragit RL-RS with TEC and HPMC with PEG 4000, respectively (Kuźmińska et al., 2021; Malebari et al., 2022). Achieving precise extrusion at relatively low temperatures is an elusive technical challenge, as it requires managing high viscosity while preventing extrusion artefacts such as oozing, stringing, and bridging, which lead to printing tailing and poor shape fidelity.

A qualified 3D printer is required for standardised production of medicines in hospital pharmacies. For pharmaceutical-grade printers to comply with good manufacturing practices (GMP), several design changes should be applied, e.g., product-contact parts material, extrusion accuracy, movement accuracy, containment from the environment, and validated software (Ahmed et al., 2025; Lafeber et al., 2024). In the last few years, a new breed of pharmaceutical-grade printers has emerged, such as M3DIMAKER for FDM, SSE, and direct extrusion (FabRx, UK), DoseRx1 for SSE (Doser, The Netherlands), Pharma Printer 1 for SSE (CurifyLabs, Finland), and Flexdose for FDM and inkjet (DiHeSys, Germany). Unlike the other 3D printers, DoseRx1 is equipped with an AISI 316 L stainless steel cartridge/syringe using the mechanical piston pressure technique, and a suitable AISI 316 L stainless steel nozzle, making this printer familiar with the SSE technique to produce 3D-printed (3DP) tablets (Ait Hoummad et al., 2025; Lyousoufi et al., 2023). In this study, the potential of this printer to manufacture accurate minitablets via direct extrusion will be explored. Even though the printhead is generally different from the ordinary single-screw extruder for direct extrusion, the mechanical pressure produced by the stainless steel printhead in the printer could be promising for extruding more viscous feedstock, which is common in low-temperature direct extrusion through a narrow nozzle. This feature plays an important role in manufacturing drug products with high accuracy and extrusion consistency.

This study proposes an alternative workflow for the accurate manufacturing of personalised minitablets via direct extrusion-based 3D printing at the point of care. We produced accurate single-unit paediatric minitablets using an SSE pharmaceutical-grade 3D printer. We employed a formulation strategy of using granules that can be extruded at relatively low temperature (70–75°C). The process parameters were optimised to enable the production of reliable, highly uniform minitablets as small as 2 mm. As a model active ingredient, carvedilol was loaded into the minitablets. In the UK, carvedilol is licensed only for adult use at doses of 3.125–25 mg (twice daily), whereas in practice it is regularly prescribed to children as an extemporaneous suspension at lower doses to treat heart failure (Chiclana-Rodríguez et al., 2023).

2. Materials and methods

2.1. Materials

Carvedilol (CAS no. 72956-09-3) was purchased from Kemprotec Ltd. (Carnforth, UK). Carvedilol film-coated tablets 12.5 mg were obtained from Milpharm Ltd. (Ruislip, UK). Eudragit E PO and Eudragit RL PO were donated by Evonik Operations GmbH (Darmstadt, Germany). Lactose monohydrate and PEG 400 were supplied by Sigma Chemical (St. Louis, USA). Glyceryl monostearate (GMS) (IMWITOR 900 K) was provided by 101 Oleochemical (Oleo GmbH) (Witten, Germany). Methanol (for HPLC, $\geq$99.9%) was purchased from Merck Life Science UK Limited (Dorset, UK). Orthophosphoric acid HiPerSolv Chromanorm® (85%) and hydrochloric acid AnalaR Normapur® (37%) were purchased from VWR International Limited (Lutterworth, UK). Anhydrous tribasic sodium phosphate was supplied from Acros Organics (New Jersey, USA). Deionised water was prepared by Elga LabWater UK Purelab® Chorus 1 (High Wycombe, UK) in King's College London (London, UK).

2.2. Preparation of the feeding powder for direct granule extrusion

All accurately weighed powder materials were transferred into a Wahl powder grinder (Kent, UK) and sheer-mixed for 1 min. Then, PEG 400 was added directly by pouring it into the pre-blended powder, and the mixture was thoroughly mixed using the powder grinder for 2 min. PEG 400 was chosen due to the greater lowering of the glass transition temperature (Tg) for some polymers, including methacrylate polymer, compared to triethyl citrate (Khodaverdi et al., 2012; Repka et al., 1999). After a wet mass (6 g) was formed, the mixture was loaded into a stainless-steel printing cartridge with a spatula. The breakdown of trialled (F1-F3) and optimised (F4-F8) minitablet formulations is detailed in Table 1. F5 was produced from licensed carvedilol tablets (12.5 mg/tablet). In many hospital environments, licensed tablets are commonly used (and sometimes preferred) as starting materials for extemporaneous preparations when API raw materials are not available due to

Table 1
Feeding powder composition of direct granule extrusion 3DP (F1-F8).

Materials	Content (%)							
	F1	**F2**	**F3**	**F4**	**F5**	**F6**	**F7**	**F8**
Carvedilol	2.5	2	2	3.5	–	6.25	7	10.5
Licensed carvedilol tablet (powder)*	–	–	–	–	43.6	–	–	–
Eudragit E	48.5	37	37	30	29.4	–	30	30
Eudragit RL	–	–	–	–	–	30	–	–
GMS	10	8	8	8	8	8	8	8
PEG 400	39	30	30	19	19	18	19	19
Lactose	–	23	–	39.5	–	37.75	36	32.5
Talc	–	–	23	–	–	–	–	–

*Each licensed carvedilol tablet (~155 mg) contains 12.5 mg carvedilol (~8% w/w).

procurement, storage, safety handling, and regulatory constraints. In this formula, the licensed tablets were crushed with a mortar and pestle, and a measured weight of Eudragit E and GMS was added. This was followed by the addition of PEG 400 as detailed above. To demonstrate a different release profile, Eudragit E in the optimised formula (F4) was replaced with an equivalent percentage of Eudragit RL (F6), with a target dose of 1.8 mg carvedilol. Higher carvedilol contents in the minitablets (2 and 3 mg per tablet) were also manufactured (F7 and F8) to investigate the uniformity.

2.3. Granule size distribution

Granule size characterisation was conducted using a Malvern Panalytical Morphologi 4 instrument (Worcestershire, UK). Samples from all mixtures were dispersed onto the glass platform using a powder dispersion unit with compressed air. Optic was set at 5× and 2.5× for mixture samples before and after mixing with PEG 400, respectively.

2.4. Rheology study

Three sets of steady-state rheology measurements were performed on the sample using a TA Instruments Discovery HR-20 instrument (New Castle, USA), with the temperature controlled by a Peltier unit. First, a viscosity curve was measured with shear rate ranging from 0.01 to 100 s^{-1} using a 20 mm parallel plate at printing temperatures (70 and 75°C for Eudragit E- and Eudragit RL-based formulations, respectively). The second measurement was performed to evaluate the thixotropy behaviour of the melted powders under conditions simulated within the syringe/cartridge at printing temperatures, using a three-interval thixotropy test (3-ITT). Those three intervals included a rest condition (low shear rate of 0.01 s^{-1} for 60 s), an "extrusion" mimicking step during which pressure was applied (high shear rate of 100 s^{-1} for 30 s), and a recovery condition (low shear rate of 0.01 s^{-1} for 60 s). The last rheology measurement, referred to as the "cooling step" test, was performed to simulate the behaviour of the melted powder after deposition on the printing platform. The test included a high shear rate of 100 s^{-1} for 30 s at the printing temperature, followed by a low shear rate of 0.01 s^{-1} for 10 min, after which the temperature was reduced to 20°C.

2.5. Direct granule extrusion 3DP process

The 3DP process involved running a JavaScript Object Notation (.json) configuration file containing printing instructions and parameters on the DoseRx1 3D printer (Leiden, The Netherlands). This file contained printing instructions, including all parameters listed in Table 2. In general, powder preparation and printing processes are illustrated in Supplementary data, Fig. S1.

The granule-filled cartridge was maintained at printing temperatures within the heated sleeve inside the printhead for 60 min before printing commenced. Cylindrical minitablets were printed from melted feeding powder through a stainless-steel nozzle with an internal diameter of 0.4 mm onto a stainless-steel printing platform covered with cellophane plastic film to prevent sticking. Extrusion was performed at 70 and 75°C for Eudragit E- and Eudragit RL-based formulations, respectively, with a speed of 10 mm/s. A batch of 10 minitablets was printed for each formulation using a layer-by-layer sequence and a predefined continuous circular (concentric) fully dense deposition path (equivalent to 100% infill). The printed tablets were then removed after 10 min to allow for complete solidification. The minitablet dimension was challenged to find the minimum weight variation (relative standard deviation, %RSD) by varying the tablet diameter (2.0–4.4 mm) and the number of printed layers (1–5) using F4 formulation.

Table 2
Printing parameters of minitablets (F1-F8).

Parameters	Value
Nozzle diameter	0.4 mm
Tablet diameter	2.0–4.4 mm (optimal diameter = 3.6 mm)
Number of layers	1–5 (optimal number of layers = 4)
Layer height	0.49 mm
Nominal density	1.41 kg/L
Retraction	11.9 mm
XY speed	10 mm/s
Cartridge temperature	70/75°C
Nozzle temperature	70/75°C

2.6. Weight measurement of 3DP minitablets

Minitablet weight was measured directly after printing using an Ohaus Adventurer Analytical AX324 balance (Nänikon, Switzerland). All measurements were performed in ten replications. The averages, standard deviations, and relative standard deviations of tablet weight were calculated.

2.7. Scanning electron microscope (SEM) imaging

The morphology of 3DP minitablets was observed using FEI Quanta 200 SEM (Hillsboro, USA) with a FEI detector and an Oxford Instruments EDS attachment (INCAx-act) (High Wycombe, UK). Samples were scanned at high vacuum (70 Pa) with a spot of 3.0 and a voltage of 10.00 kV. Samples were analysed at various magnification powers, as indicated at the bottom of each figure. The top surface and the cross-sectional area of each tablet were analysed. Samples were gold-coated with about 20 nm of Au using Quorum Technologies Emitech 550X sputter coater (Ashford, UK) at 25 mA.

2.8. Carvedilol content uniformity assay

Carvedilol content was assessed by the HPLC method, modified from British Pharmacopoeia (British Pharmacopoeia Commission, 2025a), using an Agilent 1260 Infinity equipped with an ultraviolet–visible (UV–Vis) detector (Santa Clara, USA) and an Agilent Zorbax Eclipse XDB-C8 (150 x 4.6 mm, 5 μm) column (Santa Clara, USA) as a stationary phase. A 50:50 (v/v) mixture of methanol and 0.1 M orthophosphoric acid (pH 2.0) in water was used as the isocratic mobile phase at a flow rate of 1.0 mL/min at 25°C. Each tablet was disintegrated in 50 mL mobile phase for 30 min using a GT Sonic ultrasonic bath (Guangdong, China). The mixture was then filtered through a 0.22 μm Fisher Scientific filter membrane (Massachusetts, USA) and diluted with mobile phase. Each sample solution was injected at 50 μL and measured at 285 nm. Carvedilol was eluted at approximately 5 min, with a total run time of 7 min. A set of standard solutions was also injected to plot a calibration curve over 0.05–25 μg/mL, yielding an R^2 value of 0.9996, a limit of detection (LOD) of 3.45 ng/mL, and a limit of quantification (LOQ) of 10.45 ng/mL.

2.9. Thermal analysis

Thermogravimetric analysis (TGA) was performed on approximately 10 mg of each raw material, physical mixture, and 3DP minitablet. All samples were analysed in triplicate using a TA Instruments TGA Q50 (New Castle, USA) at a heating rate of 10°C/min from 30 to 500°C with nitrogen flow rates of 40 and 60 mL/min for balance and sample, respectively. Data were analysed using TA Universal Analysis software (version 4.5A, New Castle, USA).

TA Instruments DSC 2500 (New Castle, USA) was utilised to investigate the heat flow of each material, physical mixture, and 3DP minitablet. A small portion (around 3–7 mg) of each sample was placed into a TA Instruments DSC Tzero pan with hermetic lid (New Castle, USA) and crimped promptly. Samples were heated from 10 to 170°C (except for PEG 400, −20 to 30°C, and for GMS, 10 to 150°C), at a heating rate of 10°C/min under nitrogen flow (50 mL/min). All samples were analysed in triplicate. The DSC thermograms were analysed through TA Instruments TRIOS Software version 5.1 (New Castle, USA).

2.10. X-ray diffraction (XRD)

A Rigaku PXRD MiniFlex600 (Tokyo, Japan) equipped with a D/teX Ultra2 1D advanced silicon strip detector was used to investigate the physical state of each material, the physical mixture, and 3DP minitablets. The diffractometer was operated with transmission geometry using Cu Kα radiation at 40 kV and 15 mA. The instrument was computer-controlled and analysed using Rigaku SmartLab Studio II software (version 5.2.0.3, Tokyo, Japan). Samples were mounted directly on the top of a low background silicone sample holder for measurement. Data were collected with 2θ ranging from 3° to 35°, with a step size of 1°/min and a counting time of 0.02 s per step.

2.11. In vitro drug release profile

The carvedilol dissolution method was adapted from the British Pharmacopoeia under the Carvedilol Tablets monograph for immediate-release and under Appendix XII B for modified-release (British Pharmacopoeia Commission, 2025a) and performed using an Agilent automatic dissolution apparatus 850-DS (Santa Clara, USA), with a USP II apparatus (paddle) rotating at 50 rpm. The dissolution medium consisted of 900 mL of a 0.7% hydrochloric acid solution at pH 1.5, maintained at 37 ± 0.5°C. Sample solutions were collected by an autosampler at 5, 10, 15, 20, 30, 45, and 60 min for Eudragit E-based minitablets. Dissolution samples of F6 were collected at 15, 30, 60, and 120 min in the acid medium described above, and were then collected at 2.5, 3, 4, 6, 8, 12, 18, and 24 h in a pH 6.8 medium. Each withdrawn sample was automatically replaced by an equal volume of fresh dissolution medium. All collected samples were filtered through a 0.45 μm nylon Agilent filter membrane (Santa Clara, USA) before being placed in the sample vials. The carvedilol concentration was then determined using the same HPLC procedure as the drug content uniformity assay.

2.12. Statistical analysis

One-way ANOVA and *t*-test were performed using GraphPad Prism version 10 for Windows (San Diego, USA). Differences in results less than the probability level ($p < 0.05$) were considered significant.

3. Results and discussion

This study aimed to accurately manufacture low-dose carvedilol 3DP minitablets using a simple, low-temperature direct extrusion technique with a pharmaceutical-grade 3D printer, from carvedilol raw material and licensed tablets. Low-temperature direct extrusion was chosen for this work because of its simplicity and the absence of solvent. The minitablets were produced to exhibit different release profiles using two types of Eudragit, methacrylic acid-based copolymers.

3.1. Direct granule extrusion process and formula development for 3DP minitablet

The minitablet diameter and printing layer number were optimised to achieve minimum weight variation at low carvedilol doses (1–3 mg). British National Formulary (BNF) stated that the initial dose of carvedilol in infants and children should be 0.05 mg/kg, given in two divided doses daily. The dose might be titrated at least every 2 weeks to 0.2–0.35 mg/kg daily as a maintenance dose (National Institute for Health and Care Excellence, 2026). The recommended carvedilol dose for children of different weights is summarised in Supplementary data, Table S2.

In the formula, PEG 400 was used as a plasticiser. The preblended powder was shear-mixed with PEG 400 to form granules, which were then loaded into the printing cartridge. Granule size characterisation was conducted to investigate particle-size enlargement resulting from high-shear mixing with PEG 400. All formulations exhibited particle-size enlargement (agglomeration) after mixing with PEG 400, with average sizes ranging from 76 to 198 μm (Table 3).

F1 ink exhibited sufficient flow through the nozzle at 70 and 75°C (~252 Pa.s), but did not adhere well to the base platform. At lower temperatures of 60 and 50°C, the material became too viscous (805 and 2711 Pa.s, respectively) and failed to extrude from the nozzle. However, the produced minitablets appeared to be stringing at 70 and 75°C (Supplementary data, Fig. S2A), an unwanted strand between two tablets caused by molten powder extruded during the nozzle travel between them, even with optimised retraction parameters (distance and speed). A thermostable filler was added to increase the solid content of the molten mixture, thereby improving printability and shape support (Yang et al., 2021). Lactose and talc (F2 and F3) were selected for optimisation due to their inertness and stability at the printing temperature. As a result, the printing process of the lactose-added formula (F2) showed superior shape fidelity compared to those containing talc (Supplementary data, Fig. S2B and C). Further optimisation by increasing lactose content in F4 resulted in fewer stringing defects at 70°C (Supplementary data, Fig. S2D and Video S1). Formula F5 was prepared using licensed carvedilol tablets without additional lactose. The printing process for this conversion formula also ran smoothly at 70°C, and the product appeared visually acceptable (Supplementary data, Fig. S2E). F6 with Eudragit RL was extruded well and printed at 75°C, yielding satisfactory visual results (Supplementary data, Fig. S2F). In addition, 2 mg and 3 mg carvedilol tablets (F7-F8) were produced using the optimised parameters from F4, without changing the tablet size. Both mixtures were printed smoothly at 70°C without noticeable stringing defects (Supplementary data, Fig. S2G-H).

3.2. Rheology study

The rheology of F4-F6 was explored to investigate mixture powder behaviour at each printing temperature (70°C for F4-F5 and 75°C for F6), including shear-sweep tests, three-interval thixotropy tests (3-ITT), and cooling-step tests (Fig. 1).

Flow curves measured at printing temperatures showed a decrease in viscosity with increasing shear rate for all inks (Fig. 1A). The viscosity gradually reduced during a shear rate of 0.01–10 s^{-1}, then dropped more steeply (3 magnitudes drop) at higher shear rates. This shear-thinning behaviour likely resulted from the disentanglement of polymeric chains and their alignment in the flow field, thereby reducing flow resistance and viscosity. PEG 400, as a plasticiser, also contributed to this decrease in viscosity (Bonifacio et al., 2023). This characteristic was critical for extrusion-based 3DP during printing, as it ensured the melted mixture flowed consistently under applied pressure. There was no difference in the flow curve pattern among all Eudragit types.

Viscosity curves for all types of melted ink powder mixtures over

Table 3
Particle size characterisation result (n = 3).

Parameters	F1 Powder blend	Granules*	F2 Powder blend	Granules	F3 Powder blend	Granules	F4 Powder blend	Granules	F5 Powder blend	Granules	F6 Powder blend	Granules	F7 Powder blend	Granules	F8 Powder blend	Granules
Average diameter (μm)	12.74	–	16.95	198.35	25.15	163.50	21.45	94.38	19.51	76.15	22.07	189.69	12.40	162.44	12.59	172.11
Diameter [n, 0.1] (μm)	5.68	–	5.77	4.45	9.12	8.35	5.68	20.59	6.69	8.34	5.47	8.62	5.25	4.79	5.53	4.46
Diameter [n, 0.5] (μm)	10.76	–	12.21	141.49	20.41	135.09	13.91	77.83	11.61	62.12	10.63	145.44	9.85	122.45	9.96	126.44
Diameter [n, 0.9] (μm)	20.70	–	34.14	474.37	46.79	326.83	46.20	174.55	42.14	155.85	56.16	419.25	20.64	380.40	20.60	415.66
Particles counted	33,675	–	10,634	5,708	15,623	7,373	19,634	9,744	19,178	7,806	16,479	7,058	20,437	7,093	25,623	6,707

*F1 formed large granules that could not be characterised with the instrument.

three intervals are presented in Fig. 1B. The viscosity of all compositions was initially sustained around 766–8186 Pa.s under the rest condition in the first interval. When a high shear rate of 100 s^{-1} was applied, all formulations showed a significant viscosity decline of up to 99.9% compared to the initial condition. During this stage, the viscosity of mixture F4 dropped considerably to 0.3 Pa.s. In the third (recovery) interval, all mixtures exhibited thixotropic behaviour, which can simulate the shear that the ink undergo though during the 3DP process. F4 and F5 recovered at 55–60%, while F6 exhibited a viscosity recovery of 65% within 60 s.

While the initial physical state of the pharmaceutical ink is granules, the extrusion process resembles the operational principles of SSE extrusion following the softening of the matrix at 70–75 °C. The simulation of ink deposition on the build platform is shown in Fig. 1C. When temperature control and shear were turned off (i.e., after extrusion, during ink deposition on the build platform), the viscosity recovered in two steps. In the initial stage, the internal chain structure reformed, providing the first rise in viscosity. Then, as the environment's temperature dropped approaching Tg, the mobility decreased, and the chains rearranged into better entanglements, resulting in another viscosity rise to a high final plateau (Lavygin and Chistov, 1985).

3.3. Minitablet dimension limitation challenge

To evaluate the impact of tablet dimensions on the tablet morphology and weight uniformity, the 3D printer was challenged with a set of minitablet designs by decreasing diameters and heights using optimal ink (F4). Minitablets could be printed with diameters of 2.0–4.4 mm in 1–5 layers. Fig. 2A showed that all tablets developed an appropriate cylindrical shape across the trialled size range. However, greater weight variation was observed when the tablets were printed with fewer layers (Fig. 2B). In constant-pressure extrusion, the ink flow rate remains unstable at the beginning of the printing process until it reaches a steady state (Fu et al., 2024; Wenger et al., 2022). As a result, the amount of extruded ink might vary among tablets with fewer layers. Printing three layers appeared to be the minimum number required to achieve precise tablet weight (<5% weight variation) across all investigated diameters. In this step, the optimal dimension, with the lowest RSD (1.70%), was achieved with minitablets printed in 4 layers and a diameter of 3.6 mm. The printing time for a batch of 10 minitablets with this size was 6 min 20 or 38 s per minitablet. This size was used in subsequent works in this study. The weight and content uniformity of all diameter configurations in 4 layers were also investigated.

3.4. Minitablet appearance and morphology

All formulations were then printed using the optimised size. The appearance and SEM images of the printed minitablets are displayed in Fig. 3. Fig. 3A illustrates that 3DP minitablets appeared as glossy white, cylindrical tablets across all optimised inks. A cross-sectional view of F4 minitablets revealed a uniform layer thickness of approximately 0.4 mm (Fig. 3B), which corresponded to the nozzle size. The figure also indicates that the two adjacent layers were fused, and spiral grooves were observed on the top surface (Fig. 3C) due to the printing pattern, with a width of around 0.4 mm, corresponding to the nozzle size. A minor printing tail was also observed due to the retraction movement of the printer nozzle at the end of each layer. The process exhibited high reproducibility in appearance across methacrylate polymers used in the formula.

During feeding and melting of granules, air in the intergranular spaces can become entrapped in the molten mass, leading to a porous tablet surface. These entrained bubbles can disturb pressure build-up and strand continuity during extrusion (Vajda et al., 2023). This was mitigated by introducing a preheat step for the granules in the relatively narrow stainless-steel cartridge within the heated sleeve, thereby maximising the contact area of the granules with the cartridge wall, which

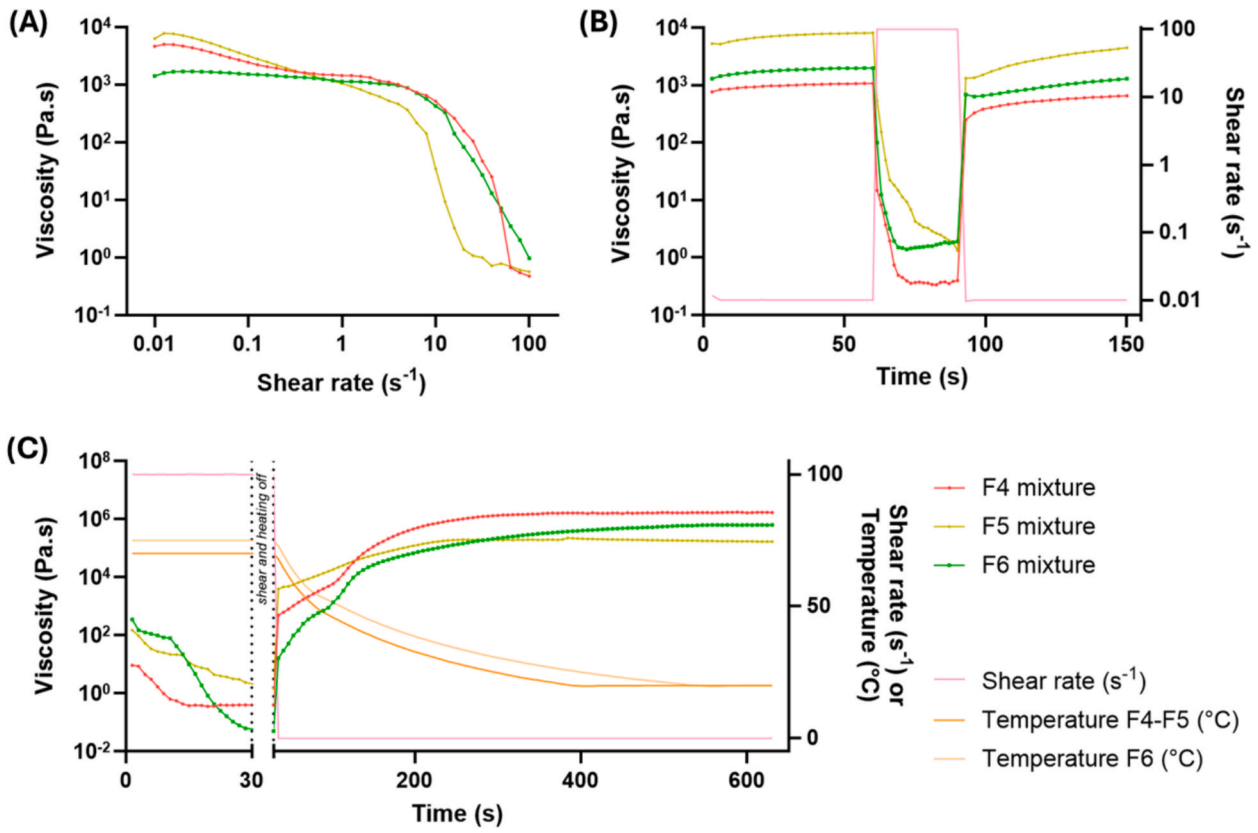

Fig. 1. (A) Flow curve with shear rate varying from 0.01 to 100 s^{-1} at printing temperatures. (B) Three interval thixotropy test (3-ITT) under low (0.01 s^{-1}), high (100 s^{-1}), and low (0.01 s^{-1}) shear rates at printing temperatures. (C) Cooling step test at high shear rate (100 s^{-1}) and printing temperatures, then switching to low shear rate (0.01 s^{-1}) with heating off.

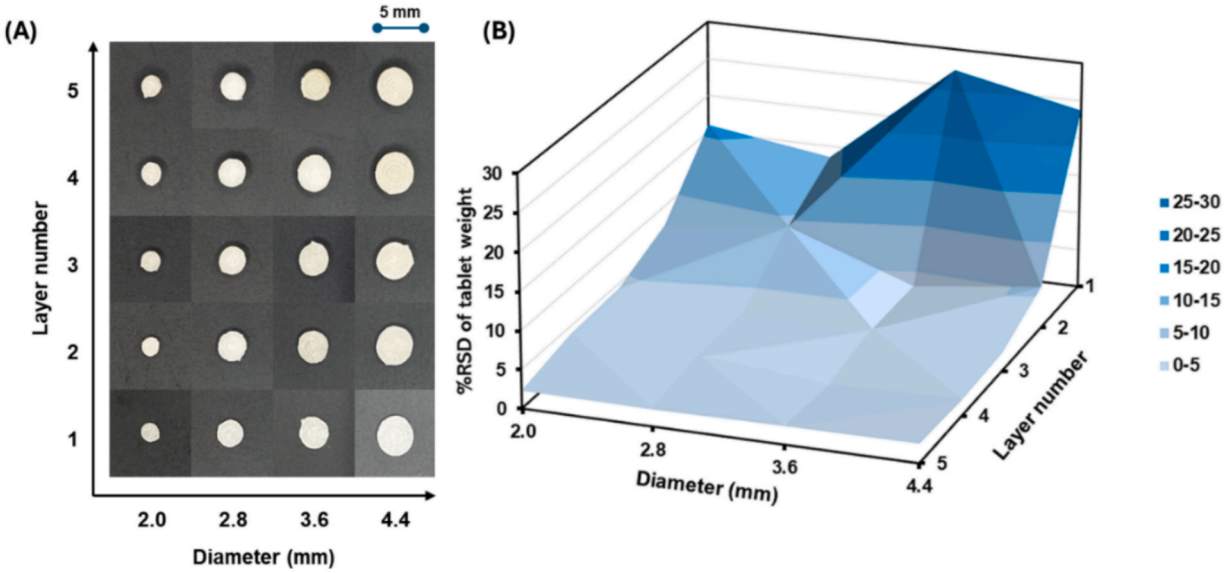

Fig. 2. (A) The appearance of 3DP minitablets in different diameters and layer numbers using F4, and (B) 3D graph of RSD percentage of the weight of minitablets (n = 10) in different investigated diameters and layer numbers.

enhance extrusion quality in heated syringe 3D printing processes (Yu et al., 2025).

3.5. Minitablet weight and carvedilol content uniformity

Minitablet weight and carvedilol content uniformity tests were performed to demonstrate printing consistency and drug distribution in the ink mixture (Table 4).

Weight uniformity across all 3DP minitablet formulations and representative size configurations revealed low variation among random samples, with RSDs as low as 1.48%, which were below the British Pharmacopoeia requirement for solid oral dosage forms of <80 mg

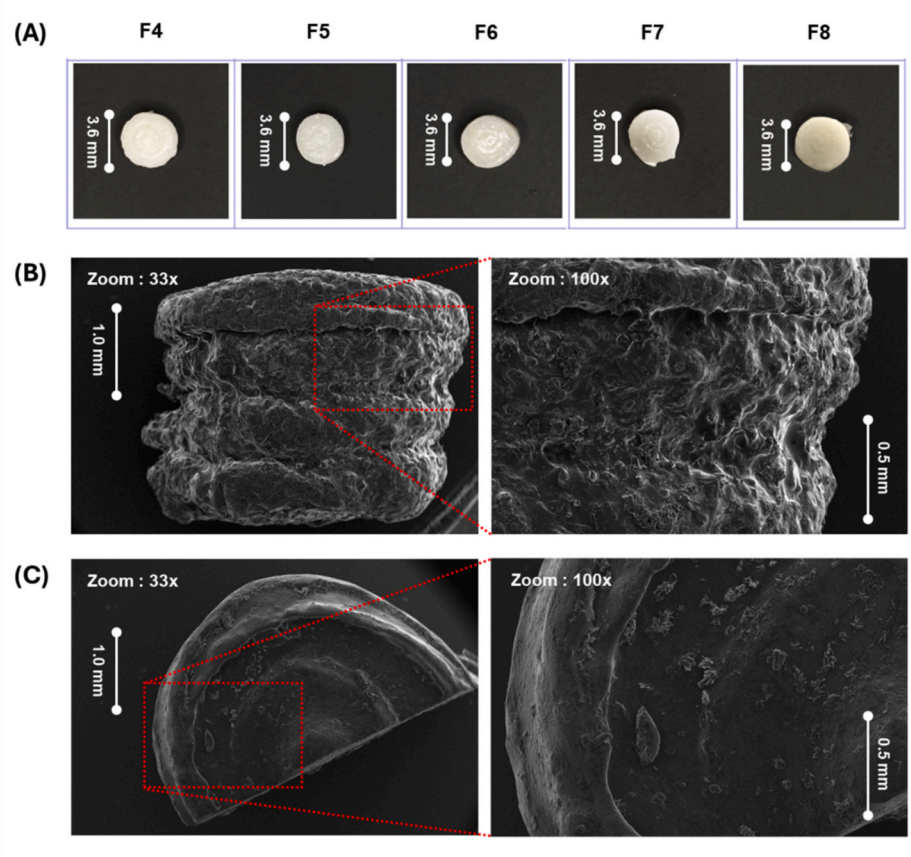

Fig. 3. (A) The appearance of 3DP minitablet's top surface across different formulations. (B) SEM images of 3DP minitablet in cross-section view and (C) top surface view with 33x and 100x magnification using F4 tablet as a representative.

Table 4
Weight and content uniformity of 3DP minitablets (n = 10) across different formulations (F4-F8) at optimum size (diameter 3.6 mm, 4 layers) and other representative size configurations.

Minitablets	Minitablet weight			Carvedilol content			
	Average (mg)	**SD (mg)**	**RSD (%)**	**Nominal (mg/tab)**	**Average (%)**	**SD (%)**	**RSD (%)**
F4, Ø 3.6 mm, 4 layers	29.15	0.47	1.60	1.0	98.15	1.94	1.98
F5, Ø 3.6 mm, 4 layers	27.81	0.97	3.48	1.0	97.44	1.13	1.16
F6, Ø 3.6 mm, 4 layers	28.17	0.42	1.48	1.8	97.34	2.61	2.68
F7, Ø 3.6 mm, 4 layers	30.02	1.10	3.67	2.0	97.44	2.25	2.31
F8, Ø 3.6 mm, 4 layers	29.59	0.81	2.74	3.0	97.80	2.31	2.36
F4, Ø 2.0 mm, 4 layers	11.14	0.45	4.00	0.3	94.99	2.52	2.66
F4, Ø 2.8 mm, 4 layers	18.59	0.60	3.22	0.6	94.37	2.77	2.94
F4, Ø 4.4 mm, 4 layers	42.73	0.88	2.06	1.5	95.52	2.10	2.20

weight (British Pharmacopoeia Commission, 2025b). Such a high level of accuracy at comparable tablet weights has been reported with DLP (Adamov et al., 2022) and DOD (Sundarkumar et al., 2023). While previous attempts at extrusion-based 3D printing technologies, such as FDM (Gorkem Buyukgoz et al., 2022; Krause et al., 2021) and SSE (Ayyoubi et al., 2025; Eduardo et al., 2021) reported a weight variation of 1.63–19.13%.

Previous studies using direct extrusion for minitablet production at 170–180°C reported higher weight variation (RSD > 5%) at comparable tablet weights (Fratini et al., 2025; Totaro et al., 2025). The employment of low tempeature mitigate the risk of thermal degradation during printing (Yang et al., 2023). The use of a compact stainless-steel syringe/cartridge (with a load capacity of only 7 g) for the DoseRx1 pharmaceutical-grade printer in this work enabled uniform heat distribution to melt the feeding powder and hold sufficient pressure to extrude a more viscous ink mass at lower temperatures. The hollow-diameter precision in the stainless-steel nozzle also contributed to the shape regularity of the molten extrudate. In addition, the piston pusher was not attached to the top piston, which directly contacted the material in the cartridge, resulting in more consistent extrusion flow and better retraction control. Such accuracy might not be achievable using heated plastic syringes, where pressure buildup and temperature distribution are common issues in material extrusion 3D printing (Díaz-Torres et al., 2022; Eichler et al., 2024; Weidenfeller et al., 2004). Nevertheless, the use of multi-use direct-material-contact parts in the 3D printer would require the hospital pharmacy to develop validated cleaning procedures to prevent cross-contamination between batches.

Carvedilol content appeared consistent for all formulations and representative size configurations. The content uniformity demonstrated high accuracy and low variation, with an average ranging from 94.4% to 98.2% of the label claim and RSDs of 1.2–2.9%, complying with the British Pharmacopoeia specification for Carvedilol Tablets (British Pharmacopoeia Commission, 2025a). These observations demonstrate the clinical potential of this direct extrusion printing

approach for producing a precisely carvedilol-dosed minitablet. It is likely that manipulating minitablet size is a more practical approach to achieving a wide dose spectrum without modifying the ink composition. Preliminary stability data showed that weight uniformity and carvedilol content remained within the pharmacopeial range for up to 9 months at ambient temperature (20–25°C) (Supplementary data, Table S1).

3.6. Thermal analysis

The thermal stability of the ingredients and 3DP minitablets was assessed by the TGA method scan from 30 to 500°C (Fig. 4). TGA profiles showed no significant weight loss with carvedilol until ~250°C (Fig. 4A), in line with a previous report (Ye et al., 2024). At the printing temperature (70–75°C), all Eudragit polymers exhibited approximately 2–3% weight loss due to water loss during heating, consistent with the material specification. In addition to Eudragit polymers, PEG 400 also showed moisture loss at below 100°C. The moisture loss in each material contributed to the weight drop of F4-F6 mixtures, losing approximately 1–2% at printing temperatures (Fig. 4B). Meanwhile, the tablet weight dropped at a slower rate below 150°C than that of the physical mixture, because they had undergone moisture loss during thermal extrusion through the direct extrusion 3D printing. All curves showed a significant drop at temperatures (material degradation) well above the processing temperature (~200°C). This confirmed that the printing temperature range (70–75°C) is appropriate for all materials used in this study.

Thermal behaviour and the effects of the printing process were also evaluated using DSC. The material thermograms (Fig. 5A) showed that carvedilol exhibited a sharp endothermic peak at 117°C, indicating its crystalline form, which was TGA-confirmed as thermally stable under 3D printing temperatures (70 and 75°C). In the mixture and tablet thermograms (Fig. 5B), two subtle endothermic peaks were observed at around 65°C and 140–155°C, corresponding to GMS and lactose monohydrate compositions, respectively. The absence of the carvedilol endothermic peak in the mixture and tablet thermograms could be attributed to its low fraction within the matrix and/or to its dissolution in PEG 400 (Ha et al., 2019).

3.7. X-ray diffraction (XRD)

To investigate the crystal behaviour of carvedilol in the 3DP minitablets, XRD profiling was performed (Fig. 6). The diffractogram from the XRD analysis (Fig. 6A) showed that carvedilol appeared to be crystalline form, with characteristic peaks at $2\theta = 5.8°$, 11.6°, 13.0°, 14.8°, 17.5°, and 18.4°, resonating with previous reported observations (Deshpande et al., 2024; Prado et al., 2014; Ye et al., 2024). Those distinctive peaks were not observable in the licensed tablet pattern, as carvedilol accounted for only ~8% of the tablet. By contrast, the lactose diffractogram, which appears in crystalline form, is dominant in the licensed tablet diffractogram, indicating a significant component in the marketed tablet. Talc also contained crystalline forms in the raw material, while broad typical peaks were observed in GMS at around $2\theta = 20–25°$. No peaks were detected in the diffractograms of all Eudragit polymers, showing an amorphous nature.

Fig. 6B showed that all physical mixtures exhibited peaks at approximately $2\theta = 20°$, indicating the presence of lactose and GMS in the formula. However, those peaks were absent in the minitablet diffractograms, indicating a transformation of the lactose form. Carvedilol peaks were not observed in either the physical-mixture or tablet graphs, possibly because it was present at a low fraction in the tablets. Therefore, it was not possible to establish the physical form of carvedilol within the minitablet matrix, consistent with the DSC results above.

3.8. In vitro drug release profile

The drug-release data for carvedilol minitablets are shown in Fig. 7. After 30 min, >80% of the drug had been released in the F4 and F5

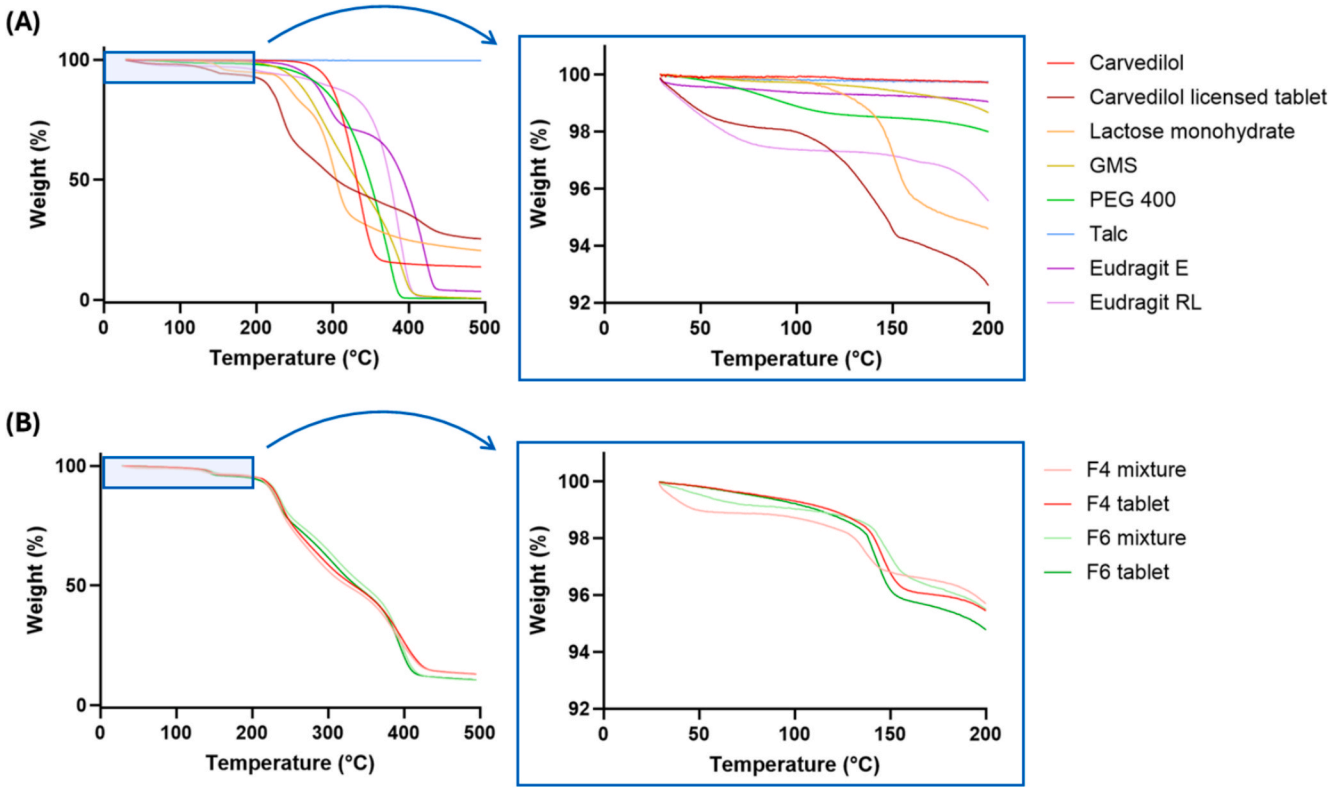

Fig. 4. TGA profiles of (A) all raw materials and (B) mixtures and tablets across different formulations, investigated at 30–500°C. The right images are magnified up to 200°C.

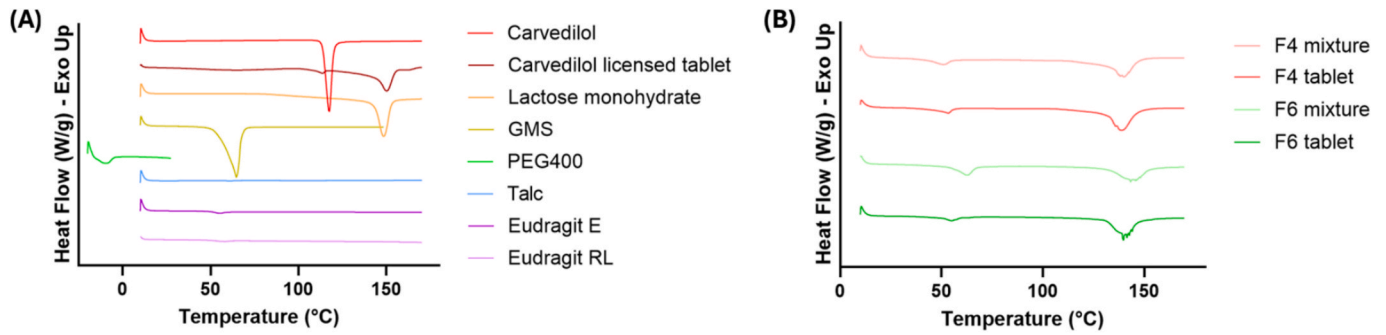

Fig. 5. DSC profiles of (A) all raw materials and (B) mixtures and tablets (F4 and F6), investigated up to 170°C.

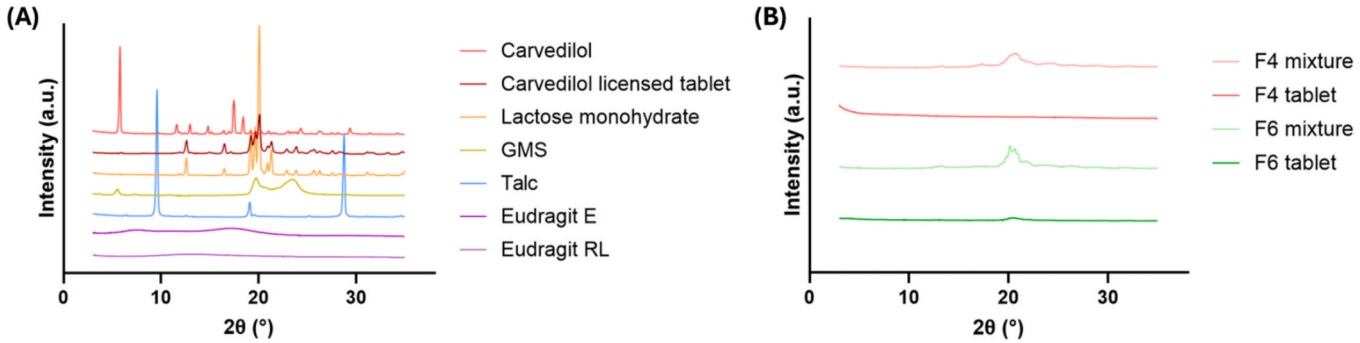

Fig. 6. XRD profile of (A) all raw materials and (B) mixtures and tablets (F4 and F6), which were investigated at 2θ = 3–35°.

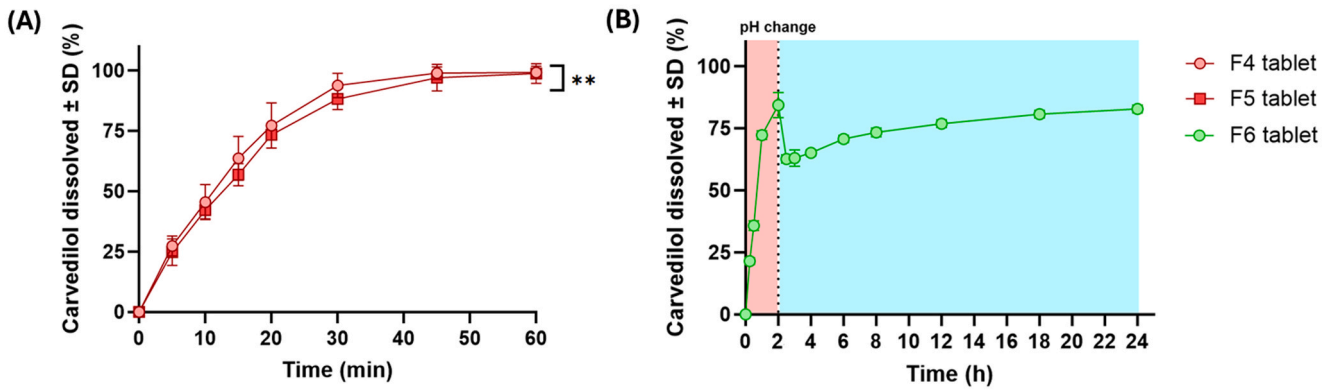

Fig. 7. (A) Drug release profile of 3DP minitablets (F4 and F5) in 60 min (n = 6). Statistical significance ($p < 0.05$) based on the paired *t*-test. ** p-value 0.001–0.01. (B) Drug release profile of 3DP minitablets (F6) in pH 1.5 for 2 h, continued to 24 h in pH 6.8 (n = 6).

formulations. This indicates that the minitablets conform to the British Pharmacopoeia requirements for Carvedilol Tablets (British Pharmacopoeia Commission, 2025a). In a simulated gastric environment, the amino group in Eudragit E is protonated, allowing hydration and dissolution of the methacrylate polymer within 30 min (Moustafine et al., 2006). This also confers an advantage for a bitter-tasting drug, as Eudragit E encapsulates the drug and prevents its dissolution in the mouth (pH ~ 7.4). As a result, the unpleasant taste does not reach the taste buds (Abdelhakim et al., 2019; Mashaqbeh et al., 2024).

Changing the polymers in the formula from Eudragit E to Eudragit RL showed dissolution retardation from 30 min (F4-5 in Fig. 7A) to 2 h (F6 in Fig. 7B), as indicated by 80% carvedilol achievement. Eudragit RL polymer is insoluble, but hydrated in aqueous medium, allowing water to penetrate and the drug to escape by diffusion through the pores or channels during polymer relaxation (Akhgari and Tavakol, 2016; Nikam et al., 2023). A significant drop was observed on F6 after the pH was adjusted from 1.2 to 6.8. This result indicates that dissolved carvedilol could be precipitated in the base-adjusted medium. Carvedilol is a weak base that is predominantly protonated and more soluble in acidic medium, whereas at higher pH, it becomes largely unionised and poorly soluble (Han et al., 2020; Loftsson et al., 2008). Even though the dose was 3 times the solubility limit at pH 6.8, precipitation might occur during the pH transition due to a sudden change in pH upon adding the phosphate buffer to the medium. Therefore, the further drug release during the buffer stage can reflect two processes: continued release from the dosage form and possible resolubilisation of the precipitate formed immediately after the pH change.

Rational design and optimisation of modified-release formulations, including geometry optimisation based on surface area-to-volume ratio and porosity, could be carried out to tune matrix hydration, diffusion pathways, and erosion, thereby achieving the desired release profile. Increasing the ratio (e.g., thinner constructs or channelled designs) generally accelerates release by increasing the exposed area and shortening the diffusion or erosion path length. 3D printing has previously

demonstrated controlled modification of geometry (diameter, thickness, and channels) to predict or intentionally shift dissolution profiles (Sadia et al., 2018; Windolf et al., 2021).

4. Conclusions

In summary, this study demonstrates that direct granule extrusion 3D printing is a feasible and reliable approach for manufacturing accurate low-dose carvedilol minitablets. Printing was performed using a pharmaceutical-grade 3D printer equipped with a high-precision stainless-steel cartridge and nozzle assembly. This study demonstrates a formulation strategy built on granule-based pharmaceutical inks that enable extrusion at relatively low processing temperatures (70–75°C). These conditions improved process robustness while minimising the risk of thermally induced drug degradation. Through process optimisation, minitablet exhibited satisfactory printing resolution, a weight-variation RSD as low as 1.48%, and content uniformity approaching that achieved with higher-resolution 3D-printing technologies.

Beyond dose accuracy, this work establishes a facile, solvent-free workflow for producing high-quality minitablets from raw materials and from licensed tablets as practical extemporaneous starting materials. The approach eliminates the need for filament manufacturing and post-print finishing, supporting the potential adoption of direct extrusion of high-accuracy personalised medicine in hospital pharmacies and at the point of care.

CRediT authorship contribution statement

Bambang V.E.B. Abdillah Akbar: Writing – original draft, Visualization, Validation, Methodology, Investigation, Formal analysis, Data curation, Conceptualization. **Michalina Seluk:** Validation, Methodology, Formal analysis, Data curation. **Abdullah Isreb:** Writing – review & editing, Resources, Methodology, Data curation. **Marcelo da Silva:** Resources, Methodology, Writing – review & editing. **Cécile A. Dreiss:** Writing – review & editing, Resources, Methodology. **Paul G. Royall:** Writing – review & editing, Resources, Methodology. **Andrea Gill:** Writing – review & editing, Conceptualization. **Louise Bracken:** Writing – review & editing, Conceptualization. **Stephen Tomlin:** Writing – review & editing, Conceptualization. **Joanna Giebułtowicz:** Writing – review & editing, Supervision. **Stuart A. Jones:** Writing – review & editing, Supervision. **Mohamed A. Alhnan:** Writing – review & editing, Supervision, Project administration, Conceptualization.

Declaration of competing interest

The authors declare the following financial interests/personal relationships which may be considered as potential competing interests: Bambang V.E.B. Abdillah Akbar reports financial support was provided by Indonesia Endowment Fund for Education. If there are other authors, they declare that they have no known competing financial interests or personal relationships that could have appeared to influence the work reported in this paper.

Acknowledgments

The research was supported by the Indonesian government through LPDP (Lembaga Pengelola Dana Pendidikan/Indonesia Endowment Funds for Education) scholarship for a PhD degree.

Appendix A. Supplementary data

Supplementary data to this article can be found online at https://doi.org/10.1016/j.ijpharm.2026.126871.

Data availability

Data will be made available on request.

References

Abdelhakim, H.E., Coupe, A., Tuleu, C., Edirisinghe, M., Craig, D.Q.M., 2019. Electrospinning optimization of Eudragit E PO with and without chlorpheniramine maleate using a design of experiment approach. Mol. Pharm. 16, 2557–2568. https://doi.org/10.1021/acs.molpharmaceut.9b00159.

Abu-Geras, D., Hadziomerovic, D., Leau, A., Khan, R.N., Gudka, S., Locher, C., Razaghikashani, M., Lim, L.Y., 2017. Accuracy of tablet splitting and liquid measurements: an examination of who, what and how. J. Pharm. Pharmacol. 69, 603–612. https://doi.org/10.1111/jphp.12671.

Adamov, I., Stanojević, G., Medarević, D., Ivković, B., Kočović, D., Mirković, D., Ibrić, S., 2022. Formulation and characterization of immediate-release oral dosage forms with zolpidem tartrate fabricated by digital light processing (DLP) 3D printing technique. Int. J. Pharm. 624, 122046. https://doi.org/10.1016/j.ijpharm.2022.122046.

Aguilar-de-Leyva, Á., Casas, M., Ferrero, C., Linares, V., Caraballo, I., 2024. 3D printing direct powder extrusion in the production of drug delivery systems: state of the art and future perspectives. Pharmaceutics 16, 437. https://doi.org/10.3390/pharmaceutics16040437.

Ahmed, A.A., Schimmel, K.J.M., Tubic-Grozdanis, M., Tuleu, C., Smith, J., Soulairol, I., Dadkhah, A., Paulson, M., Lechanteur, A., Carrez, L., Schnor, T., Lagarce, F., Le Brun, P.P.H., Crauste-Manciet, S., 2025. Expert opinion on extrusion-based pharmaceutical 3D printing from the European Society of Hospital Pharmaceutical Technology (GERPAC). Int. J. Pharm. 686, 126321. https://doi.org/10.1016/j.ijpharm.2025.126321.

Aina, M., Baillon, F., Sescousse, R., Sanchez-Ballester, N.M., Begu, S., Soulairol, I., Sauceau, M., 2025. From conception to consumption: applications of semi-solid extrusion 3D printing in oral drug delivery. Int. J. Pharm. 674, 125436. https://doi.org/10.1016/j.ijpharm.2025.125436.

Ait Hoummad, A., Ramcharan, A., Shokri, F., 2025. Stability assessment of a novel 3D-printed oral dosage form of Mexiletine Hydrochloride: a six-month shelf-life study. Pharm. Dev. Technol. 30, 1525–1534. https://doi.org/10.1080/10837450.2025.2590122.

Akhgari, A., Tavakol, A., 2016. Prediction of optimum combination of eudragit RS/eudragit RL/ethyl cellulose polymeric free films based on experimental design for using as a coating system for sustained release theophylline pellets. Adv. Pharm. Bull. 6, 219–225. https://doi.org/10.15171/apb.2016.030.

Auel, T., Mentrup, A.F.C., Oldfield, L.R., Seidlitz, A., 2025. 3D printing of pharmaceutical dosage forms: recent advances and applications. Adv. Drug Deliv. Rev. 217, 115504. https://doi.org/10.1016/j.addr.2024.115504.

Ayyoubi, S., Holst, A., Maduro, J., Van der Kuy, P., Van Ee, R., Van de Velde, D., Valkenburg, B., Hennep, C., Quodbach, J., Ruijgrok, E., 2025. Benchmarking pharmaceutical quality and manufacturing costs of 3D printing against conventional compounding methods for personalization of medicine. Eur. J. Pharm. Sci. 212, 107180. https://doi.org/10.1016/j.ejps.2025.107180.

Bernatoniene, J., Stabrauskiene, J., Kazlauskaite, J.A., Bernatonyte, U., Kopustinskiene, D.M., 2025. The future of medicine: how 3D printing is transforming pharmaceuticals. Pharmaceutics 17, 390. https://doi.org/10.3390/pharmaceutics17030390.

Bonifacio, A., Bonetti, L., Piantanida, E., De Nardo, L., 2023. Plasticizer design strategies enabling advanced applications of cellulose acetate. Eur. Polym. J. 197, 112360. https://doi.org/10.1016/j.eurpolymj.2023.112360.

British Pharmacopoeia Commission, 2025a. Carvedilol Tablets, in: British Pharmacopoeia. TSO (The Stationery Office).

British Pharmacopoeia Commission, 2025b. Appendix II C. Consistency of Formulated Preparations, in: British Pharmacopoeia. TSO (The Stationery Office).

Chiclana-Rodríguez, B., Garcia-Montoya, E., Rouaz-El Hajoui, K., Romero-Obon, M., Nardi-Ricart, A., Suñé-Pou, M., Suñé-Negre, J.M., Pérez-Lozano, P., 2023. Development of a carvedilol oral liquid formulation for paediatric use. Pharmaceutics 15, 2283. https://doi.org/10.3390/pharmaceutics15092283.

Cui, M., Pan, H., Su, Y., Fang, D., Qiao, S., Ding, P., Pan, W., 2021. Opportunities and challenges of three-dimensional printing technology in pharmaceutical formulation development. Acta Pharm. Sin. B 11, 2488–2504. https://doi.org/10.1016/j.apsb.2021.03.015.

Deshpande, A., Mer, V., Patel, D., Thakkar, H., 2024. Microneedle-assisted transdermal delivery of carvedilol nanosuspension for the treatment of hypertension. RSC Pharmaceutics 1, 472–483. https://doi.org/10.1039/D4PM00038B.

Díaz-Torres, E., Rodríguez-Pombo, L., Ong, J.J., Basit, A.W., Santoveña-Estévez, A., Fariña, J.B., Alvarez-Lorenzo, C., Goyanes, A., 2022. Integrating pressure sensor control into semi-solid extrusion 3D printing to optimize medicine manufacturing. Int. J. Pharm. X 4, 100133. https://doi.org/10.1016/j.ijpx.2022.100133.

Duncan, J.C., Page, R., Clark, J., Seddon, G., Slater, J., Gill, A., Dliso, S., Ohia, U., Skoutelis, N., Wagner-Hattler, L., Baumgartner, A., Sprunk, A., Kühl, P., Bracken, L., 2026. Acceptability of minitablets in soft food. A randomised cross-over study in children. Front. Pharmacol. 16. https://doi.org/10.3389/fphar.2025.1702183.

Eduardo, D.-T., Ana, S.-E., José, B.F., 2021. A micro-extrusion 3D printing platform for fabrication of orodispersible printlets for pediatric use. Int. J. Pharm. 605, 120854. https://doi.org/10.1016/j.ijpharm.2021.120854.

Eichler, F., Balc, N., Bremen, S., Nink, P., 2024. Investigation of laser powder bed fusion parameters with respect to their influence on the thermal conductivity of 316L

samples. J. Manufact. Mater. Process. 8, 166. https://doi.org/10.3390/jmmp8040166.
EMA, 2013. Guideline on pharmaceutical development of medicines for paediatric use [WWW Document]. https://www.ema.europa.eu/en/documents/scientific-guideline/guideline-pharmaceutical-development-medicines-paediatric-use_en.pdf.
Flemming, J., Mielck, J.B., 1995. Requirements for the production of microtablets: suitability of direct-compression excipients estimated from powder characteristics and flow rates. Drug Dev. Ind. Pharm. 21, 2239–2251. https://doi.org/10.3109/03639049509065904.
Fratini, C., Moroni, S., Angelis, D.D., Tiboni, M., Balducci, A.G., Rossi, A., Aluigi, A., Amadei, F., Casettari, L., 2025. Direct powder extrusion (DPE) 3D-printing of mini-tablets for preclinical studies in rodents. Int. J. Pharm. 675, 125542. https://doi.org/10.1016/j.ijpharm.2025.125542.
Fu, Z., Angeline, V., Sun, W., 2024. Evaluation of printing parameters on 3D extrusion printing of pluronic hydrogels and machine learning guided parameter recommendation. Int. J. Bioprint. 7, 434. https://doi.org/10.18063/ijb.v7i4.434.
Galande, A.D., Khurana, N.A., Mutalik, S., 2020. Pediatric dosage forms—challenges and recent developments: a critical review. J. Appl. Pharm. Sci. 155–166. https://doi.org/10.7324/JAPS.2020.10718.
Ghazali, H.S., Askari, E., Seyfoori, A., Naghib, S.M., 2023. A high-absorbance water-soluble photoinitiator nanoparticle for hydrogel 3D printing: synthesis, characterization and in vitro cytotoxicity study. Sci. Rep. 13, 8577. https://doi.org/10.1038/s41598-023-35865-3.
Gorkem Buyukgoz, G., Kossor, C.G., Ji, S., Guvendiren, M., Davé, R.N., 2022. Dose titration of solid dosage forms via FDM 3D-printed mini-tablets. Pharmaceutics 14, 2305. https://doi.org/10.3390/pharmaceutics14112305.
Ha, E.-S., Kim, J.-S., Lee, S.-K., Sim, W.-Y., Jeong, J.-S., Kim, M.-S., 2019. Equilibrium solubility and solute-solvent interactions of carvedilol (form I) in twelve mono solvents and its application for supercritical antisolvent precipitation. J. Mol. Liq. 294, 111622. https://doi.org/10.1016/j.molliq.2019.111622.
Han, H., Li, Y., Peng, Z., Long, K., Zheng, C., Wang, W., Webster, T.J., Ge, L., 2020. A Soluplus/Poloxamer 407-based self-nanoemulsifying drug delivery system for the weakly basic drug carvedilol to improve its bioavailability. Nanomedicine 27, 102199. https://doi.org/10.1016/j.nano.2020.102199.
Hu, J., Fitaihi, R., Abukhamees, S., Abdelhakim, H.E., 2023. Formulation and characterisation of carbamazepine orodispersible 3D-printed mini-tablets for paediatric use. Pharmaceutics 15, 250. https://doi.org/10.3390/pharmaceutics15010250.
Kaba, K., Purnell, B., Liu, Y., Royall, P.G., Alhnan, M.A., 2023. Computer numerical control (CNC) carving as an on-demand point-of-care manufacturing of solid dosage form: A digital alternative method for 3D printing. Int. J. Pharm 645, 123390. https://doi.org/10.1016/j.ijpharm.2023.123390.
Kachrimanis, K., Petrides, M., Malamataris, S., 2005. Flow rate of some pharmaceutical diluents through die-orifices relevant to mini-tableting. Int. J. Pharm. 303, 72–80. https://doi.org/10.1016/j.ijpharm.2005.07.003.
Kakkilaya, A., Shahzad, M., Bourgeois, F.T., 2025. FDA approval of orphan drug indications for pediatric patients, 2011-2023. JAMA Pediatr. 179, 203. https://doi.org/10.1001/jamapediatrics.2024.5280.
Kasahun, A.E., Sendekie, A.K., 2023. Are pediatrics taking the prescribed tablet dosage form? Practices of off-label tablet modification in pediatric wards: a prospective observational study. Heliyon 9, e15109. https://doi.org/10.1016/j.heliyon.2023.e15109.
Khan, D., Kirby, D., Bryson, S., Shah, M., Mohammed, A.R., 2022. Paediatric specific dosage forms: patient and formulation considerations. Int. J. Pharm. 616, 121501. https://doi.org/10.1016/j.ijpharm.2022.121501.
Khodaverdi, E., Tekie, F.S.M., Amoli, S.S., Sadeghi, F., 2012. Comparison of plasticizer effect on thermo-responsive properties of eudragit RS films. AAPS PharmSciTech 13, 1024–1030. https://doi.org/10.1208/s12249-012-9827-y.
Kim, G.-T., Go, H.-B., Yu, J.-H., Yang, S.-Y., Kim, K.-M., Choi, S.-H., Kwon, J.-S., 2022. Cytotoxicity, colour stability and dimensional accuracy of 3D printing resin with three different photoinitiators. Polymers (Basel) 14, 979. https://doi.org/10.3390/polym14050979.
Klingmann, V., Spomer, N., Lerch, C., Stoltenberg, I., Frömke, C., Bosse, H.M., Breitkreutz, J., Meissner, T., 2013. Favorable acceptance of mini-tablets compared with syrup: a randomized controlled trial in infants and preschool children. J. Pediatr. 163, 1728–1732.e1. https://doi.org/10.1016/j.jpeds.2013.07.014.
Krause, J., Müller, L., Sarwinska, D., Seidlitz, A., Sznitowska, M., Weitschies, W., 2021. 3D printing of mini tablets for pediatric use. Pharmaceuticals 14, 143. https://doi.org/10.3390/ph14020143.
Kuźmińska, M., Pereira, B.C., Habashy, R., Peak, M., Isreb, M., Gough, T.D., Isreb, A., Alhnan, M.A., 2021. Solvent-free temperature-facilitated direct extrusion 3D printing for pharmaceuticals. Int. J. Pharm. 598, 120305. https://doi.org/10.1016/j.ijpharm.2021.120305.
Lafeber, I., de Boer, T.W.J., van Unen, W.H., Ouwerkerk, N., Guchelaar, H.J., Schimmel, K.J.M., 2024. Design of a pharmaceutical 3D printer using quality-by-design approach. J. Pharm. Innov. 19, 87. https://doi.org/10.1007/s12247-024-09889-9.
Lavygin, I.A., Chistov, S.F., 1985. Temperature dependence of the viscosity of polymer melts and liquid-liquid transitions. Polym. Sci. U.S.S.R. 27, 1478–1485. https://doi.org/10.1016/0032-3950(85)90296-5.
Lennartz, P., Mielck, J.B., 1998. Minitabletting: improving the compactability of paracetamol powder mixtures. Int. J. Pharm. 173, 75–85. https://doi.org/10.1016/S0378-5173(98)00206-3.
Liu, Y., Leonova, A.M., Royall, P.G., Abdillah Akbar, B.V.E.B., Cao, Z., Jones, S.A., Isreb, A., Hawcutt, D.B., Alhnan, M.A., 2023. Laser-cutting: A novel alternative approach for point-of-care manufacturing of bespoke tablets. Int. J. Pharm. 647, 123518. https://doi.org/10.1016/j.ijpharm.2023.123518.
Loftsson, T., Vogensen, S.B., Desbos, C., Jansook, P., 2008. Carvedilol solubilization and cyclodextrin complexation: a technical note. AAPS PharmSciTech 9, 425–430. https://doi.org/10.1208/s12249-008-9055-7.
Loo, S.J., Seah, X.Y., Heng, P.W.S., Chan, L.W., 2023. Study of diminutive granules as feed powders for manufacturability of high drug load minitablets. Int. J. Pharm. 638, 122922. https://doi.org/10.1016/j.ijpharm.2023.122922.
Lura, V., Lura, A., Breitkreutz, J., Klingmann, V., 2025. The revival of the mini-tablets: recent advancements, classifications and expectations for the future. Eur. J. Pharm. Biopharm. 210, 114655. https://doi.org/10.1016/j.ejpb.2025.114655.
Lyousoufi, M., Lafeber, I., Kweekel, D., de Winter, B.C.M., Swen, J.J., Le Brun, P.P.H., Bijleveld-Olierook, E.C.M., van Gelder, T., Guchelaar, H., Moes, D.J.A.R., Schimmel, K.J.M., 2023. Development and bioequivalence of 3D-printed medication at the point-of-care: bridging the gap toward personalized medicine. Clin. Pharmacol. Ther. 113, 1125–1131. https://doi.org/10.1002/cpt.2870.
Malebari, A.M., Kara, A., Khayyat, A.N., Mohammad, K.A., Serrano, D.R., 2022. Development of advanced 3D-printed solid dosage pediatric formulations for HIV treatment. Pharmaceuticals 15, 435. https://doi.org/10.3390/ph15040435.
Mashaqbeh, H., Obaidat, R.M., Alsmadi, M.M., 2024. Solvent-free method for masking the bitter taste of azithromycin dihydrate using supercritical fluid technology. Drug Dev. Ind. Pharm. 50, 102–111. https://doi.org/10.1080/03639045.2023.2298892.
Meruva, S., Singaraju, A.B., Vinjamuri, B.P., Ternik, R., Stagner, W.C., 2024. Current state of minitablet product design: a review. J. Pharm. Sci. 113, 1123–1154. https://doi.org/10.1016/j.xphs.2024.02.016.
Meyers, R.S., 2024. The past, present, and future of oral dosage forms for children. J. Pediatric Pharmacol. Therapeutics 29, 22–31. https://doi.org/10.5863/1551-6776-29.1.22.
Milliken, R.L., Quinten, T., Andersen, S.K., Lamprou, D.A., 2024. Application of 3D printing in early phase development of pharmaceutical solid dosage forms. Int. J. Pharm. 653, 123902. https://doi.org/10.1016/j.ijpharm.2024.123902.
Miyazaki, K., Hida, N., Kamiya, T., Yamazaki, T., Murayama, N., Kuroiwa, M., Kurata, N., Ishikawa, Y., Yamashita, S., Nakamura, H., Nakamura, A., Harada, T., 2022. Comparative acceptability of mini-tablets, fine granules, and liquid formulations in young children: an exploratory randomized crossover study. J. Drug Deliv. Sci. Technol. 70, 103154. https://doi.org/10.1016/j.jddst.2022.103154.
Moustafine, R.I., Zaharov, I.M., Kemenova, V.A., 2006. Physicochemical characterization and drug release properties of Eudragit® E PO/Eudragit® L 100-55 interpolyelectrolyte complexes. Eur. J. Pharm. Biopharm. 63, 26–36. https://doi.org/10.1016/j.ejpb.2005.10.005.
National Institute for Health and Care Excellence, 2026. Carvedilol [WWW Document]. BNF for Children.
Neves, I., Auxtero, M.D., 2021. Dosing accuracy of oral extemporaneous suspensions of antibiotics: measuring procedures and administration devices. Pharmaceutics 13, 528. https://doi.org/10.3390/pharmaceutics13040528.
Nikam, A., Sahoo, P.R., Musale, S., Pagar, R.R., Paiva-Santos, A.C., Giram, P.S., 2023. A systematic overview of Eudragit® based copolymer for smart healthcare. Pharmaceutics 15, 587. https://doi.org/10.3390/pharmaceutics15020587.
Paulsson, M., Hamre Svendsen, R., Andersen, J.K.N., Kälvemark Sporrong, S., Andersson, Y., Tho, I., 2025. Challenges and considerations in manipulating oral dosage forms in paediatric healthcare settings: a narrative review. Acta Paediatr. https://doi.org/10.1111/apa.70199.
Prado, L.D., Rocha, H.V.A., Resende, J.A.L.C., Ferreira, G.B., de Figuereido Teixeira, A.M. R., 2014. An insight into carvedilol solid forms: effect of supramolecular interactions on the dissolution profiles. CrstEngComm 16, 3168–3179. https://doi.org/10.1039/C3CE42403K.
Protopapa, C., Siamidi, A., Kolipaka, S.S., Junqueira, L.A., Douroumis, D., Vlachou, M., 2024. In vitro profile of hydrocortisone release from three-dimensionally printed paediatric mini-tablets. Pharmaceutics 16, 385. https://doi.org/10.3390/pharmaceutics16030385.
Repka, M.A., Gerding, T.G., Repka, S.L., McGinity, J.W., 1999. Influence of plasticizers and drugs on the physical-mechanical properties of hydroxypropylcellulose films prepared by hot melt extrusion. Drug Dev. Ind. Pharm. 25, 625–633. https://doi.org/10.1081/DDC-100102218.
Rouaz, K., Chiclana-Rodríguez, B., Nardi-Ricart, A., Suñé-Pou, M., Mercadé-Frutos, D., Suñé-Negre, J.M., Pérez-Lozano, P., García-Montoya, E., 2021. Excipients in the paediatric population: a review. Pharmaceutics 13, 387. https://doi.org/10.3390/pharmaceutics13030387.
Sadia, M., Arafat, B., Ahmed, W., Forbes, R.T., Alhnan, M.A., 2018. Channelled tablets: an innovative approach to accelerating drug release from 3D printed tablets. J. Control. Release 269, 355–363. https://doi.org/10.1016/j.jconrel.2017.11.022.
Spomer, N., Klingmann, V., Stoltenberg, I., Lerch, C., Meissner, T., Breitkreutz, J., 2012. Acceptance of uncoated mini-tablets in young children: results from a prospective exploratory cross-over study. Arch. Dis. Child. 97, 283–286. https://doi.org/10.1136/archdischild-2011-300958.
Sundarkumar, V., Wang, W., Nagy, Z., Reklaitis, G., 2023. Manufacturing pharmaceutical mini-tablets for pediatric patients using drop-on-demand printing. Int. J. Pharm. 644, 123355. https://doi.org/10.1016/j.ijpharm.2023.123355.
Taylor, Z.L., Green, F.G., Hossain, N., Burckart, G.J., Pacanowski, M., Schuck, R.N., 2024. Assessment of dosing strategies for pediatric drug products. Clin. Pharmacol. Ther. 116, 716–723. https://doi.org/10.1002/cpt.3250.
Totaro, M., Racaniello, G.F., Lopalco, A., Lopedota, A.A., Denora, N., 2025. Development of 3D-printed captopril mini-tablets with customized release profiles for paediatric hypertension therapy. Int. J. Pharm. 678, 125685. https://doi.org/10.1016/j.ijpharm.2025.125685.

Vajda, J., Banović, L., Miško, M., Drstvenšek, I., Milojević, M., Maver, U., Vihar, B., 2023. Algorithmic linearization improves syringe-based extrusion in elastic systems using hydrogel-based materials. Mater. Des. 229, 111884. https://doi.org/10.1016/j.matdes.2023.111884.

Waterman, K.C., Adami, R.C., 2005. Accelerated aging: prediction of chemical stability of pharmaceuticals. Int. J. Pharm. 293, 101–125. https://doi.org/10.1016/j.ijpharm.2004.12.013.

Weidenfeller, B., Höfer, M., Schilling, F.R., 2004. Thermal conductivity, thermal diffusivity, and specific heat capacity of particle filled polypropylene. Compos. A Appl. Sci. Manuf. 35, 423–429. https://doi.org/10.1016/j.compositesa.2003.11.005.

Wenger, L., Strauß, S., Hubbuch, J., 2022. Automated and dynamic extrusion pressure adjustment based on real-time flow rate measurements for precise ink dispensing in 3D bioprinting. Bioprinting 28, e00229. https://doi.org/10.1016/j.bprint.2022.e00229.

Windolf, H., Chamberlain, R., Quodbach, J., 2021. Predicting drug release from 3D printed oral medicines based on the surface area to volume ratio of tablet geometry. Pharmaceutics 13, 1453. https://doi.org/10.3390/pharmaceutics13091453.

Yang, T.L., Stogiannari, M., Janeczko, S., Khoshan, M., Lin, Y., Isreb, A., Habashy, R., Giebułtowicz, J., Peak, M., Alhnan, M.A., 2023. Towards point-of-care manufacturing and analysis of immediate-release 3D printed hydrocortisone tablets for the treatment of congenital adrenal hyperplasia. Int. J. Pharm. 642, 123072. https://doi.org/10.1016/j.ijpharm.2023.123072.

Yang, Y., Wang, H., Xu, X., Yang, G., 2021. Strategies and mechanisms to improve the printability of pharmaceutical polymers Eudragit® EPO and Soluplus®. Int. J. Pharm. 599, 120410. https://doi.org/10.1016/j.ijpharm.2021.120410.

Ye, L., Furuishi, T., Yamashita, T., Yonemochi, E., 2024. Characterization and crystal structural analysis of novel carvedilol adipate and succinate ethanol-solvated salts. Molecules 29, 4704. https://doi.org/10.3390/molecules29194704.

Yu, K.Y., Goo, D.Y., Lee, I.H., 2025. Research on the extrusion characteristics for the geometry of materials in material extrusion process using heating syringe. Sci. Rep. 15, 11292. https://doi.org/10.1038/s41598-025-88512-4.

Zuccari, G., Alfei, S., Marimpietri, D., Iurilli, V., Barabino, P., Marchitto, L., 2022. Mini-tablets: a valid strategy to combine efficacy and safety in pediatrics. Pharmaceuticals 15, 108. https://doi.org/10.3390/ph15010108.